Heating of the core of active regions

Durgesh Tripathi

Helen Mason, James Klimchuk

Active region structure

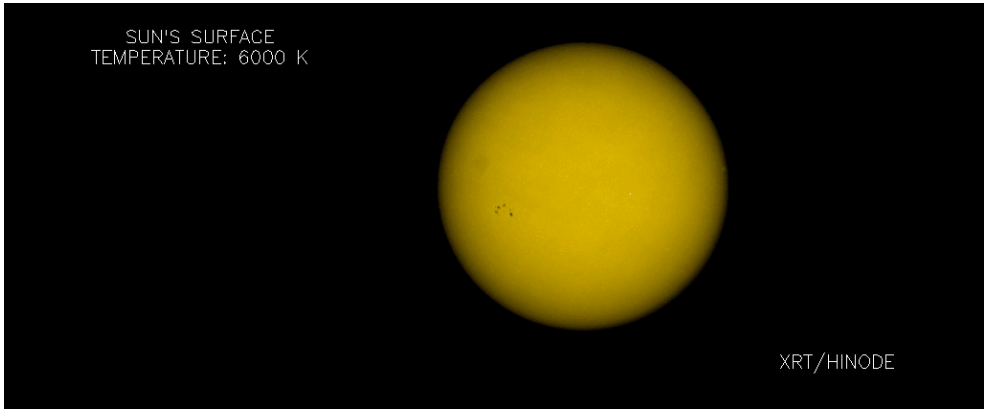

There are different varieties of loop structures in Active Regions. Are they all heated by a single process OR they are heated by a completely different mechanisms?

Heating of the warm loops

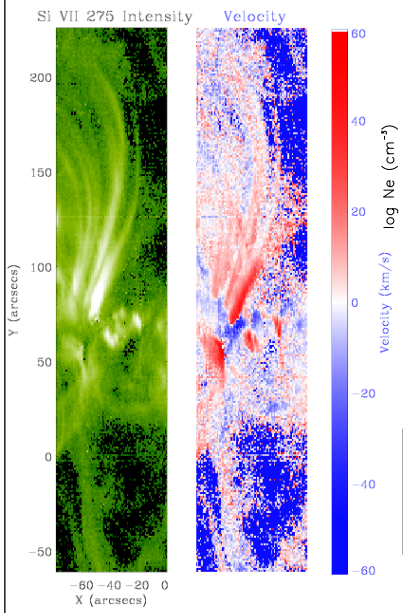

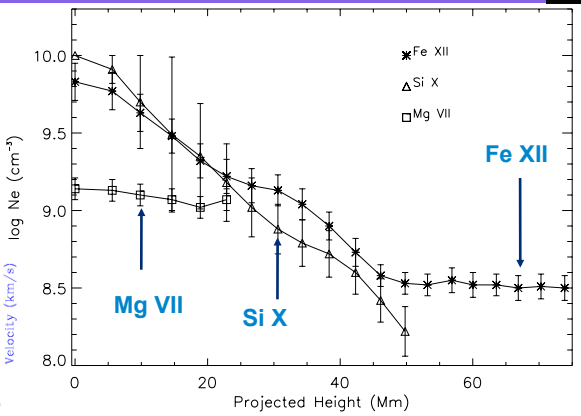

Measured properties of warm loops appear to be consistent with multi-stranded nanoflare heated loops.

Tripathi et al. 2009, ApJ

How about the heating in hot core loops?

It is difficult to resolve one specific loop in the core of active regions.

The present instruments are not with adequate spatial resolution!

The solar corona at higher temperature is inherently fuzzier.

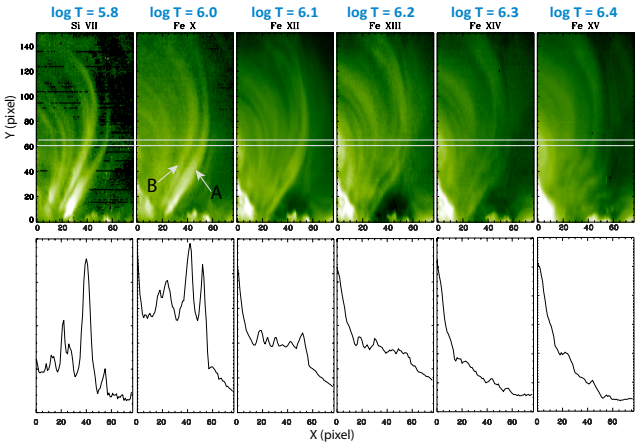

Tripathi et al. 2009, ApJ

Heating of the hot core loops

Active Region moss are the footpoints of hot core loops (Berger et al. 1999; Schrijver et al. 1999, Martens et al. 2000, Tripathi et al. 2010a)

Diagnostics of plasma in moss and inter-moss region can tell us a great deal about the heating of hot core loops.

From Tripathi et al. 2010a

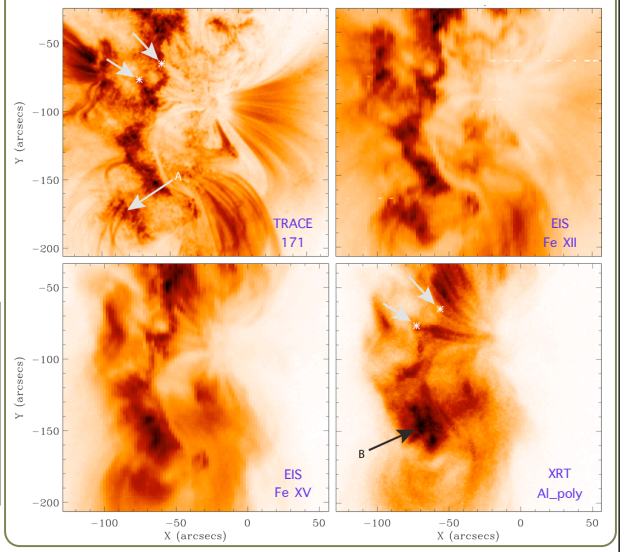

Diagnostic of the moss plasma

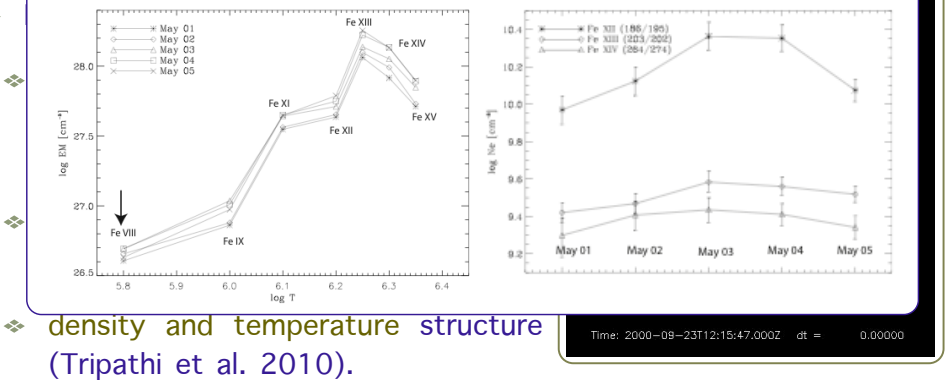

- density and temperature structure (Tripathi et al. 2010).

Antiochos et al. 2003

Predicted intensities using steady heating match quite well with observed intensities IF an expansion at the foot-points of loops are assumed (Warren et al. 2010).

Moss is time variable on a small scale. However global structure remains unchanged.

Hinode EIS observations

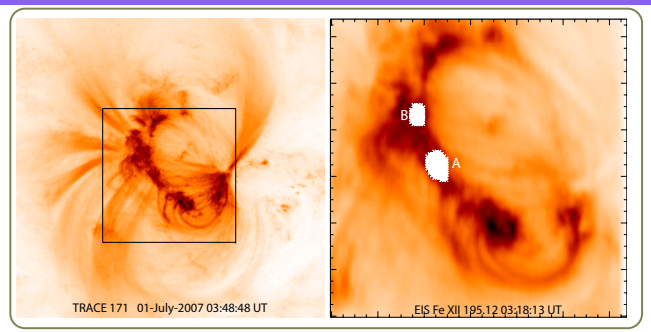

- Date: 01-Jul-2007, Full EIS Spectrum [170-210 Å, 250-190 Å]
- Exposure time: 25 sec, 1 arc sec slit; FOV: 128” x 128”

We derived EM(T) in regions A and B and compared with EM(T) derived by Klimchuk et al. (2008).

Observed EM(T)

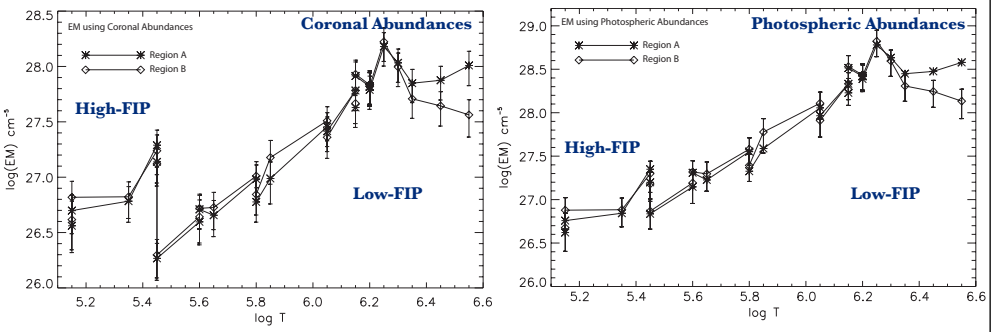

- The EM(T) for two different moss regions are strikingly similar.
- The EMs obtained using photospheric abundances are consistent for different ions.

Klimchuk et al. 2008 EBTEL

- Strong evaporation: the heat flux from the corona far exceeds the radiative losses from the transition region. The energy balance is then between thermal conduction heating and enthalpy cooling.
- Strong condensation: the heat flux from the corona much less than the radiative cooling. The energy balance is then between enthalpy heating and radiative cooling.
- Static Equilibrium: the heat flux from the corona very nearly balances the radiative losses from the transition region.

Theoretical EM(T): Klimchuk et al.(2008)

$$EM_{se} \approx ln(10) \left(\frac{\kappa_0}{14}\right)^{1/2} \frac{\bar{P}\, T^{3/4}}{k\, \Lambda(T)^{1/2}} \; ... \; static\ equilibrium$$

$$EM_{con} \approx - ln(10) \frac{5\, k\, J_0\, T}{\Lambda(T)} \; ... \; strong\ condensation$$

$$EM_{ev} \approx \frac{ln(10)}{20} \frac{\kappa_0}{k^3} \frac{\bar{P}^2\, T^{1/2}}{J_0} \; ... \; strong\ evaporation$$

k_0 = 1.6 x 10^{-6} CGS
k = Boltzmann's constant
T =Temperature
J0 = mass flux = **n v**
n = electron number density
v = plasma flow speed
Λ(T) = Optically thin radiative loss function (from CHIANTI v 6.0)

These expressions provide EM curves for individual strands.

We have considered average pressure (P) and mass flux (J0) as arbitrary constants.

We have restricted ourselves only with temperature dependence of EM curves.

Observed vs theoretical EM(T)

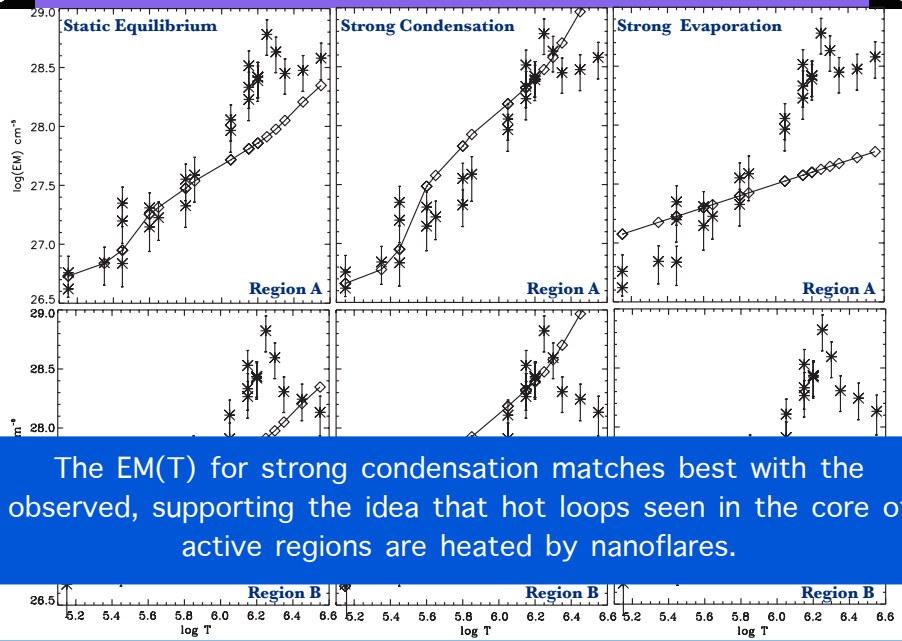

The EM(T) for strong condensation matches best with the observed, supporting the idea that hot loops seen in the core of active regions are heated by nanoflares.

Observations of Inter-moss regions

Warren et al 2011

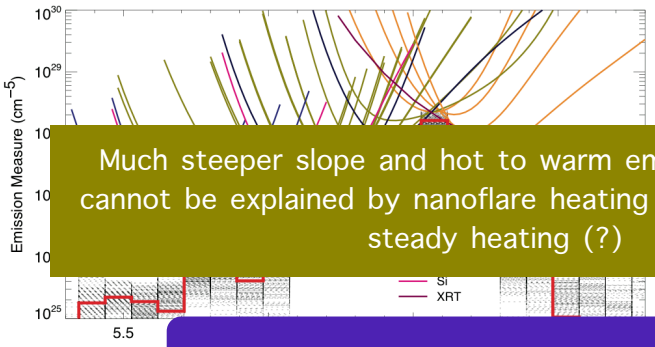

Slope of the curve towards lower temperature = 3.2

Much steeper slope and hot to warm emission ratio, that cannot be explained by nanoflare heating (?). Suggestive of steady heating (?)

How common is this?

- Emission measure of inter-moss region is strongly peaked at log T = 6.6 and falls off sharply at both ends.
- Ratio of EM at log T = 6.6 to log T = 5.8 is 400.
- Similar results were obtained by Winebarger et al. (2011)

Inter-moss regions

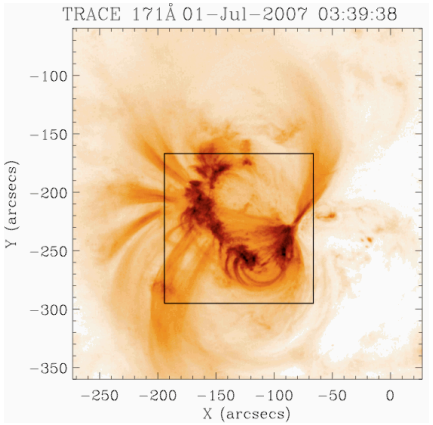

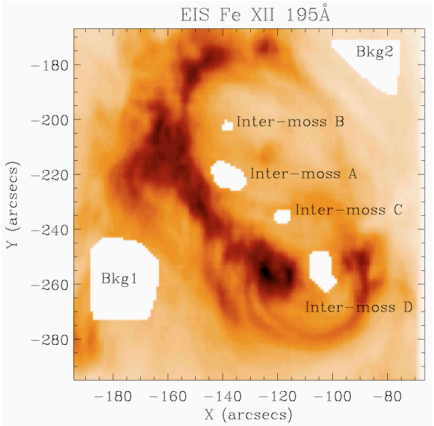

Visual inspection

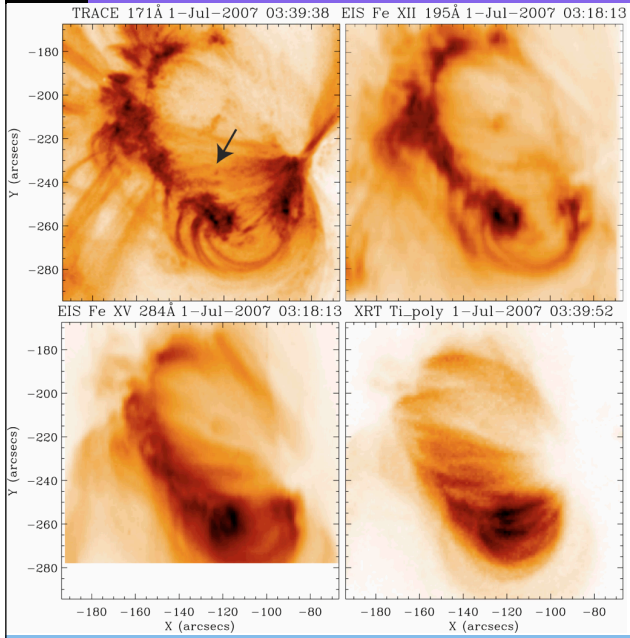

Clear signature of co-spatial hot and warm emission in the core of active region.

The emission is in form of both a diffuse component and distinct loops.

EM-Loci and $EM_{Pottasch}$

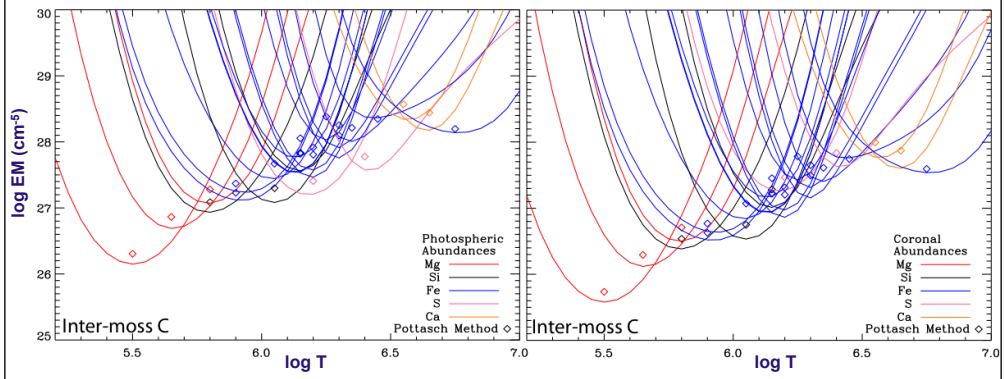

EM(T) in the inter-moss regions are more consistent with Coronal Abundances.

For the same active regions, in Moss regions, EM(T) was more consistent with Photospheric Abundances.

EM(T) Distribution

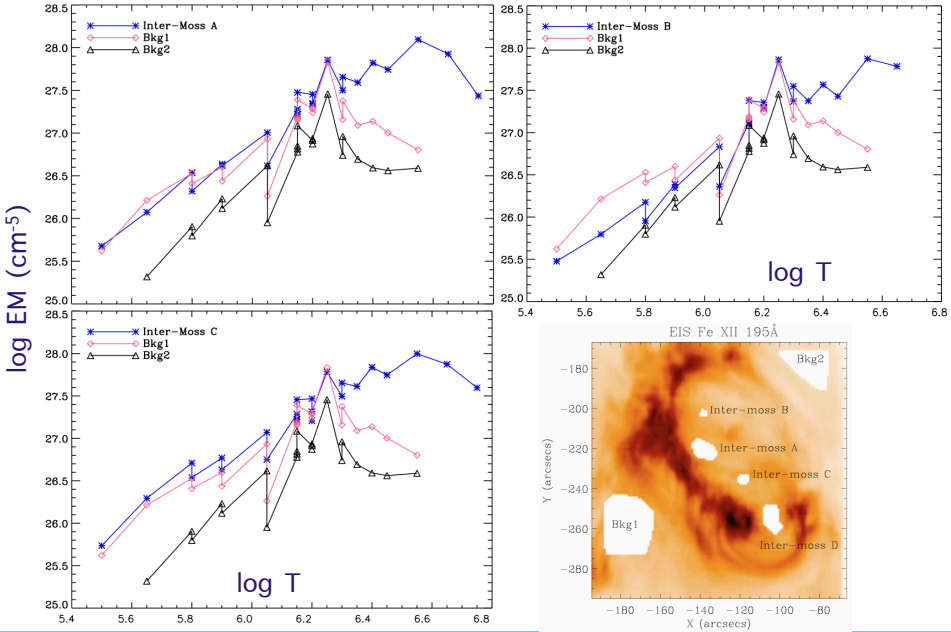

Background Estimation

We feel that considering either Bkg1 or Bkg2 will be overestimation of background.

Lower lying plasma is denser and brighter due to gravitational stratification.

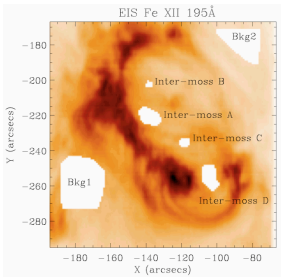

Ratio of integrated EM above height z with integrated EM above photosphere would be:

$$\frac{EM(z)}{EM(0)} = \exp\left(-\frac{2z}{H_n}\right)$$

Hn is scale height

arcade width = 6×10^4 km
Height = 3×10^4km
For TRACE:
Hn = 3×10^4 km
Reduction factor = 0.14

Warms loops are known to have density scale height larger than a factor of 2. Hn = 6×10^4 km => reduction factors = 0.4

Slopes of EM(T) curves

Regions	Optimum Foreground	No foreground	Severe Foreground	EM_{hot}/EM_{warm}
Inter-moss A	2.39±0.14	2.33±0.15	2.35±0.13	45
Inter-moss B	2.64±0.22	2.47±0.22	2.70±0.25	62
Inter-moss C	2.11±0.13	2.08±0.14	2.05±0.14	23
Inter-moss D	2.17±0.15	2.14±0.14	2.13±0.17	37
AR10980	−−	2.33±0.19	−−	69

These slopes are lower then those obtained by Winebarger et al. 2011 (3.2) and Warren et al. 2011 (3.26) much lower ratio than that obtained by Warren et al. 2011 (400).

Modelling: EBTEL Simulations

Loop half length = 2.4×10^9 cm; Duration of nanoflare = 500s,
Amplitude = 0.04 erg cm^{-3} s^{-1}, Repetition time = every 8000s
Constant low level heating = 10^{-6} erg cm^{-3} s^{-1}

The time average energy flux needed to maintain the column is 3.75×10^6 erg cm^{-2} s^{-1} (Withbroe and Noyes 1977)

Data points are the average of the EM of regions A,B, C subtracted by the average of EM for Bkg1 and Bkg2 reduced by a factor 4.

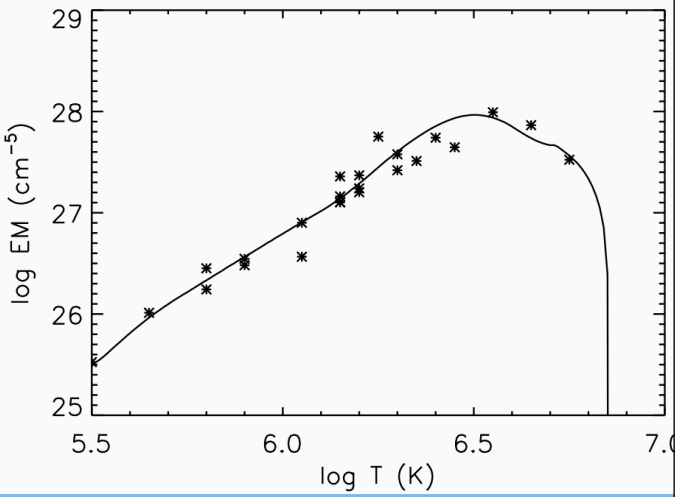

Observed and Predicted Intensities

Ion Name	Wavelength (Å)	log T (K)	Observed Intensity	Predicted Intensity
Mg V	276.58	5.50	6.7	7.3
Mg VI	268.99	5.65	7.3	8.5
Si VII	275.36	5.80	42.4	62.7
Mg VII	278.40	5.80	48.5	41.2
Fe IX	197.86	5.90	36.0	51.3
Fe IX	188.50	5.90	72.8	107.4
Si IX	258.08	6.05	26.6	59.7
Fe X	184.54	6.05	238.2	256.2
Fe XI	180.41	6.15	823.6	909.4
Fe XI	188.23	6.15	492.8	475.5
Fe XI	188.30	6.15	299.9	181.73
Si X	261.04	6.15	89.6	97.9
Fe XII	192.39	6.20	258.9	344.9
Fe XII	195.12	6.20	872.9	1072.3
S X	264.15	6.20	72.0	64.9
Fe XIII	202.04	6.25	676.4	359.3
Fe XIV	270.52	6.30	325.7	479.6
Fe XIV	274.20	6.30	636.8	661.9
Fe XV	284.16	6.35	5452.9	7680.6
S XIII	256.69	6.40	492.8	482.0
Fe XVI	262.98	6.45	443.2	448.7
Ca XIV	193.87	6.55	108.4	66.9
Ca XV	200.97	6.65	55.3	38.0
Fe XVII	269.42	6.75	6.0	9.0

Predicted intensities are within 20-30% of the observed intensities.

Conclusions

Observed emission both from "moss" and "inter-moss" regions can be explained by a simple nano-flare heated loop models.

EM(T) in the moss regions is more consistent with photospheric abundances while that in the inter-moss regions is more consistent with coronal abundances.

It should be noted that the same active region observed at the same time using the same observational sequence provides clues for two different set of abundances. Fractionation of the elements, therefore, may hold some important information which could be used to constrain the coronal heating theories.

References

Tripathi, D., Mason, H.E., et al. 2009, ApJ, 694, 1256

Tripathi, D., Mason, H.E., et al. 2010, A&A, 518, 42

Tripathi, D., Mason, H.E., Klimchuk, J. A. 2010, ApJ, 723, 713

Tripathi, D., Klimchuk, J. A., Mason, H. E., 2011, ApJ, in press